Molecular Crystals and Liquid Crystals Science and Technology. Section A. Molecular Crystals and Liquid Crystals

Publication details, including instructions for authors and subscription information:
http://www.tandfonline.com/loi/gmcl19

Enhanced Phase-Matched Second-Harmonic Generation in a Ferroelectric Liquid Crystal Waveguide

V. S. U. Fazio [a b], V. Zauls [c], S. Schrader [c], P. Busson [d], A. Hult [d], S. T. Lagerwall [a] & H. Motschmann [b]

[a] Department of Microelectronics and Nanoscience, Liquid Crystal Physics, Chalmers University of Technology & Göteborg University, S-41296, Göteborg, Sweden

[b] Max-Plank-Institute of Colloids and Interfaces, D-14476, Golm/Potsdam, Germany

[c] Institue of Physics, Univeristy of Potsdam, D-14469, Potsdam, Germany

[d] Department of Polymer Technology, Royal Institute of Technology, SE-10044, Stockholm, Sweden

Version of record first published: 24 Sep 2006

Mol. Cryst. and Liq. Cryst., 2001, Vol. 368, pp. 293-302
Reprints available directly from the publisher
Photocopying permitted by license only

Enhanced Phase-Matched Second-Harmonic Generation in a Ferroelectric Liquid Crystal Waveguide

V.S.U. FAZIO[ab], V. ZAULS[c], S. SCHRADER[c], P. BUSSON[d], A. HULT[d], S.T. LAGERWALL[a] and H. MOTSCHMANN[b]

[a]*Department of Microelectronics and Nanoscience, Liquid Crystal Physics, Chalmers University of Technology & Göteborg University, S-41296 Göteborg, Sweden,* [b]*Max-Plank-Institute of Colloids and Interfaces, D-14476 Golm/Potsdam, Germany,* [c]*Institue of Physics, Univeristy of Potsdam, D-14469 Potsdam, Germany and* [d]*Department of Polymer Technology, Royal Institute of Technology, SE-10044 Stockholm, Sweden*

A binary mixture of crosslinkable ferroelectric liquid crystals (FLCs) was used for the design of a channel waveguide. The liquid crystal was aligned in layers parallel to the glass plates (homeotropic) in a sandwich geometry and then the arrangement was permanently fixed by photopolymerization which yielded a polar network possessing a high thermal and mechanical stability. The linear and nonlinear optical properties have been measured and all four independent components of the nonlinear susceptibility tensor d have been determined. The off-resonant d-coefficients are remarkably high and comparable to those of the best known inorganic materials. Phase-matching was achieved by taking advantage of the modal dispersion of the waveguide. A reversal of sign of $\chi^{(2)}$ at the nodal plane of the electric field distribution of the first-order mode was needed to maximize the overlap integral between the fundamental and the second-harmonic (SH) light. In samples with $\chi^{(2)}$ inversion the SH signal was 1000 larger that in samples without $\chi^{(2)}$ inversion.

Keywords: Second-harmonic generation; phase-matching; $\chi^{(2)}$ inversion; crosslinkable ferroelectric liquid crystals

INTRODUCTION

The figure of merit of all devices based on second-harmonic effects is given by the ratio d_{eff}^2/n^3, where d_{eff} is the effective reduced nonlinear optical susceptibility and n the refractive index of the material. A high conversion efficiency requires the simultaneous maximization of many parameters and quite often there is a trade-off between some properties. A crucial quantity is $\chi^{(2)}$ which is, subject to certain simplifying assumptions, proportional to the number density of the NLO chromophores and to the orientational average of the hyperpolarizabilities [1]. Hence, a maximization of d_{eff} requires a chromophore with a large value of β arranged in a uniform fashion with a high degree of polar order and a high number density. These demands can be fulfilled by ferroelectric liquid crystals (FLCs). Their molecular symmetry allows a local dipolar order perpendicular to the director [2] which can be extended to the whole sample either by orienting all the molecular dipoles in an external electric field or by surface constraints [3].

Phase-matching can be achieved by taking advantage of the modal dispersion of the waveguide [4]. The effective refractive index n_{eff} of a mode is a function of waveguide thickness and polarization. Thus, phase-matching requires the fabrication of a waveguide of a precisely defined thickness given by the linear optical constants. Also, due to the dispersion of the refractive index, phase-matching is only possible between modes of different order. However, even if this is achieved, the resulting efficiency may still be rather low due to the small value of the overlap integral of the electric field distribution of the interacting modes across the cross-sectional area [4]

$$\mathcal{I} = \int_0^\infty \frac{\chi^{(2)}{}_{ijk}}{\chi^{(2)}{}_{\text{eff}}} E_i^{(m',\omega)}(z)\, E_j^{(m',\omega)}(z)\, E_k^{(m,2\omega)}(z)\, dz, \qquad (1)$$

where $\chi^{(2)}{}_{ijk}$ is the second-order susceptibility tensor, $\chi^{(2)}{}_{\text{eff}}$ is the effective second-order susceptibility, and $E_i^{(m',\omega)}(z)$ is the electric field distribution of the m'-th mode of frequency ω across the waveguide thickness. Field distributions of modes of different order yield a nearly vanishing overlap integral and a poor conversion efficiency [4]. A way out of this dilemma is to influence the susceptibility tensor [5]. A reversal of sign of $\chi^{(2)}$ at the nodal plane of the electric field distribution of the first-order mode maximizes the value of the overlap integral and thus enables a phase-matching scheme $\text{TM}_0{}^\omega$–$\text{TE}_1{}^{2\omega}$ and $\text{TE}_0{}^\omega$–$\text{TE}_1{}^{2\omega}$. The sign of $\chi^{(2)}$ can be reversed by reversing the polar order of the chromophores.

MATERIAL AND SAMPLE PREPARATION

In this work we used a mixture of the two FLCs shown in Figure 1 together with its absorption spectrum. A mixture composed by 60 % **A1b** and 40 %

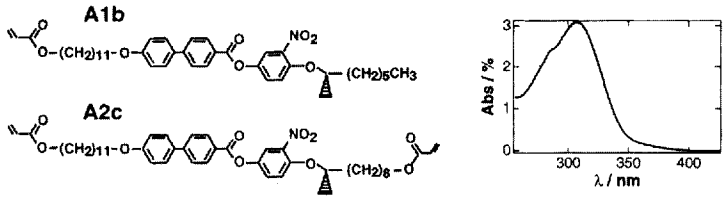

(a) (b)

Figure 1: (a) FLC monomers used in this experiment. (b) Absorption spectrum of the mixture A1b/A2c 60/40 in chloroform solution 0.13 mM.

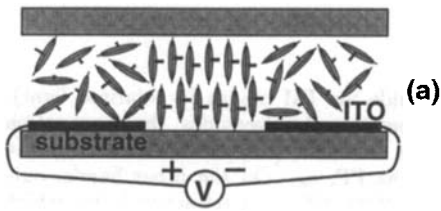

Figure 2: Cross section of a cell. In the gap between the electrodes (100 μm wide) the FLC material is oriented by the AC/DC field. The dipole moments are aligned along the cell plates perpendicular to the electodes stripe and in the channel between the electrodes we have a macroscopic polarization.

A2c is used which adopts at room temperature a chiral smectic C phase [6] with large spontaneous polarization ($P_s = [190 \pm 20]\,\mathrm{nC\,cm^{-2}}$ at 24°C [7]). The two FLC monomers are functionalized with polymerizable groups. A very small quantity of the photoinitiator Lucirin TPO (BASF) was added to the mixture to enable photopolymerization.

The FLC monomers were homeotropically oriented between planar electrodes (100 μm gap) as shown in Figure 2. They were first oriented by a DC electric field and then illuminated with UV-light. Photopolymerization leads to the formation of a thermally and mechanically stable polymer network [6–10] where the polar order between the electrodes is frozen (pyroelectric polymer, PP). A micrograph of a cell after polymerization is shown in Figure 3. Rotation of the sample about the normal to the glass plates (z-axis) did not change any features between the cross polarisers, which means that the macroscopic optic axis is parallel to z.

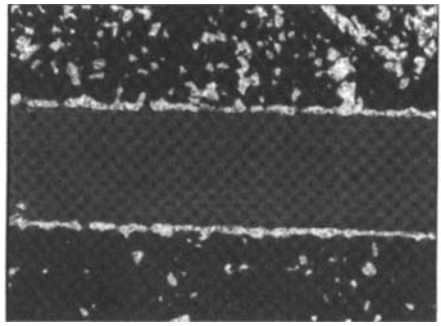

Figure 3: Micrograph of a cell between crossed polarizers after polymerization. The PP molecules are uniformally oriented in the channel between the electrodes. The cell thickness is 13 μm and the electrode gap is 100 μm.

OPTICAL CHARACTERIZATION

Waveguide losses

The structure is a channel waveguide for TM modes (p-polarised light). Assuming homeotropic alignment between the electrodes, the propagation characteristics of TM modes in the channel region are dominated by the extraordinary refractive index of the PP, n_e. On the other hands, outside the channel region p-polarised light will see a refractive index which is somewhere in between n_e and n_o. Since $n_e > n_o$ at all wavelengths (the values n_e and n_o are reported in the caption of Figure 4), TM modes are three-dimensionally confined in the channel region and no additional preparation processes are required to obtain this desired feature. Homeotropic geometry is thus advantageous: the corresponding arrangement in planar cells, where the alignment is uniform in the whole cell, leads only to slab waveguides.

The losses for p-polarised light at 1064 nm were measured by monitoring the output power at different lengths of the guide [7]. *End-fire* coupling was used to excite waveguide modes. The loss coefficient was found to be

$$\alpha = (1.07 \pm 0.95) \text{ dB cm}^{-1}. \quad (2)$$

The upper limit of the losses is on the order of 2 dB/cm which meets already the demands imposed by nonlinear optical devices.

Nonlinear optical characterization

SHG requires noncentrosymmetry and thus can only occur within the channel region of our waveguide where the FLC helix is unwound and the PP is macroscopically polar. The unwound SmC* liquid crystal phase belongs to the C_2 symmetry group [11]. In the homeotropic geometry only TE-to-TE

d_{22}	=	(0.76 ± 0.10) pm V^{-1}
d_{16}	=	(0.63 ± 0.09) pm V^{-1}
d_{23}	=	(1.26 ± 0.16) pm V^{-1}
d_{14}	=	(0.13 ± 0.02) pm V^{-1}

Table 1: The four independent d-coefficients as calculated from the fits in Figure 4.

(s-to-s) or TM-to-TE (p-to-s) conversions are allowed [12]. The effective susceptibilities which govern the conversions can be expressed in terms of the components of the four independent componenets of the nonlinear optical susceptibility tensor $\overline{d}$ as:

$$\text{TE-to-TE} \qquad d_{\text{eff}} = d_{22}, \tag{3}$$

$$\text{TM-to-TE} \qquad d_{\text{eff}} = d_{16}\cos^2\theta + d_{23}\sin^2\theta + 2d_{14}\sin\theta\cos\theta, \tag{4}$$

where θ is the fundamental light incidence angle at the glass/polymer interface. The d-coefficients can be estimated measuring the SH signal as a function of the fundamental light incidence angle. This measurement was performed in transmission using a YAG laser (1064 nm, 35 ps, 10 Hz). The results are shown in Figure 4 and the estimated d-coefficients are listed in table 1. The values are comparable to those of quartz due to the large molecular hyperpolarizabilities combined with the high degree of orientational order and the high number density of the active chromophores in our system.

PHASE-MATCHING EXPERIMENT

The desired inverted waveguide structure can be fabricated using the sandwich geometry shown in Figure 2. The top plate of a 540 nm thick cell was removed. No damage occurred in this preparation process (the mean roughness is on the order of few nanometers as confirmed by atomic force microscopy [7]). The bottom plate with the polymer network was cut in two pieces of equal size ($\approx$ 4 mm) and the parts were glued onto each other with inverse polarities in the channel region as illustrated in Figure 5.

Waveguide modes were excited by *end-fire* coupling. The laser source was a tunable OPG/OPA system pumped by the third harmonic of a Nd-YAG laser (energy per pulse $\sim$ 30 mJ, pulse duration 35 ps). The second-harmonic (SH) light was collected at the end of the guide and measured as a function of the fundamental light wavelength with a photomultiplier. The linear constants and the thickness of the waveguide were measured prior to the experiment and used to predict the wavelengths at which phase-matching occurs. According to these data and with a total cell thickness of 2×540 nm, TE–TE phase-matching should occur at 958 nm and TM–TE phase-matching at 1311 nm. These predictions were confirmed by the experiment: TE–TE phase-matching was observed at 955 nm and TM–TE

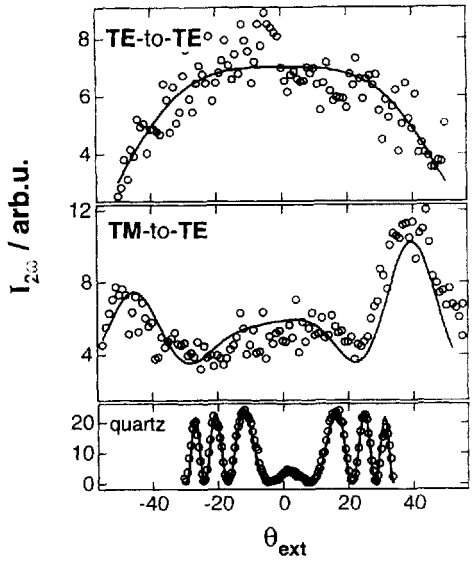

Figure 4: Second-harmonic light intensity versus external angle of incidence for s-to-s and p-to-s conversions, and for the quartz crystal of reference. The dots are the experimental values and the lines correspond to fits according to [13], with the following parameters: glass plate refractive indices, $n_g(\omega) = 1.46$ and $n_g(2\omega) = 1.50$; FLC ordinary refractive indices, $n_o(\omega) = 1.47$ and $n_o(2\omega) = 1.52$ [6]; FLC extraordinary refractive indices, $n_e(\omega) = 1.57$ and $n_e(2\omega) = 1.62$ [6]; cell thickness $13\,\mu$m; second-order susceptibility of the quartz used for calibration, $d_{11} = (0.32 \pm 0.04)$ pm V^{-1} [14]. The values of the second-order reduced susceptibilities calculated from the fits are listed in Table 1.

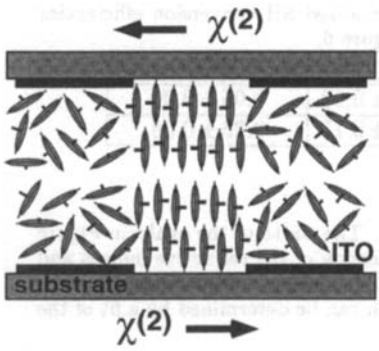

Figure 5: Scheme of the $\chi^{(2)}$-inverted structure. $\chi^{(2)}$ undergoes an abrupt sign reversal at half the total thickness of the cell. Cell thickness is 2×540 nm.

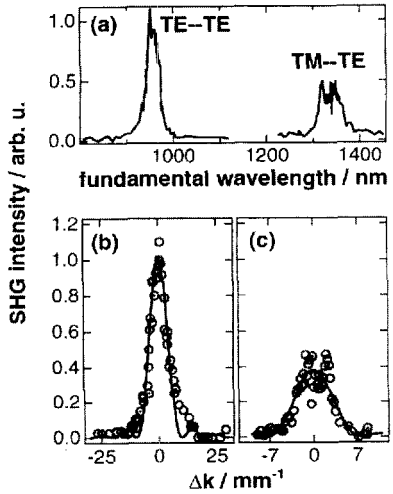

Figure 6: (a) Phase-matching peaks as a function of the fundamental light wavelength. (b) TE_0^{ω}–$TE_0^{2\omega}$ phase-matching peak at 955 nm, data and fit. (c) TM_0^{ω}–$TE_0^{2\omega}$ phase-matching peak at 1337 nm, data and fit.

Table 2: Interaction lengths and normalized SH conversion efficiencies for the two phase-matching peaks in Figure 6.

phase-matched modes	L [mm]	η [% W^{-1} cm^{-2}]
$TE_0{}^{\omega} - TE_1{}^{2\omega}$	0.59 ± 0.08	0.05 ± 0.02
$TM_0{}^{\omega} - TE_1{}^{2\omega}$	0.82 ± 0.15	0.26 ± 0.06

at 1337 nm, as shown in Figure 6(a) [15]. The width of the peaks in Figure 6(b) and (c) depends on the known dispersion of the refractive indices and on the interaction length L in which fundamental and second harmonic light are in phase. The interaction length can be determined by a fit of the experimental data to the function

$$I_{2\omega} \propto \mathrm{sinc}^2\left(\frac{L\,\Delta k}{2}\right), \tag{5}$$

where $\Delta k = 4\pi[n_{\mathrm{eff}}(2\omega) - n_{\mathrm{eff}}(\omega)]/\lambda_{\omega}$, with L as the only unknown parameter. Figures 6(b) and (c) present the experimental data together with the corresponding fits. The interaction lengths are listed in Table 2. In a sample with $\chi^{(2)}$-inversion at the phase-matching condition the SH signal was about 1000 times larger than that of an not-inverted sample, which demonstrates the superior performance due to the optimization of the overlap integral in our geometry. The normalised conversion efficienciency

$$\eta = \frac{P_{2\omega}}{P_{\omega}{}^2 L^2} \tag{6}$$

of the two phase-matching schemes is also given in Table 2. The confinement of TM modes three-dimensionally in the waveguide yields a larger conversion efficiency for TM–TE than for TE–TE phase-matching.

CONCLUSIONS

The demonstration of true phase matching in a waveguide format using FLCs is a major step towards a more general use of these materials for NLO devices. FLCs maximize the possible number density of active chromophores and this, together with a high degree of orientation, leads to remarkably high values of the off-resonant nonlinear susceptibilities. Phase-matching was achieved between modes of different order using the modal dispersion of the waveguide. Applying the concept of an inverted structure [5] maximizes the overlap integral and thus enables high efficiency in the desired phase matching-scheme. We have successfully manufactured a macroscopic inverted waveguide and demonstrated phase-matching. The quasi-homeotropic alignment avoids the use of aligning layers and leads

to an inherent channel waveguide for TM modes without any additional preparation steps, yielding a very high normalized conversion efficiency for TM–TE phase-matching scheme. Another major feature is that the order of the monomeric FLC is made permanent by photopolymerization. The photopolymerization does not lead to any degradation of the quality of the waveguide, as it is for instance observed in LB films [16]. Apparently the intrinsic fluidity of FLC heals all distortions caused by the formation of new bonds. The polar network is thermally and mechanically stable and all samples kept their NLO properties over the monitored period of several months. Thus, the system has the potential to achieve practical levels of performance.

ACKNOWLEDGMENTS

The authors are grateful to Prof. H. Möhwald for generous support and encouraging discussions. V. S. U. Fazio and S. T. Lagerwall are grateful to the TMR European Programme (contract number ERBFMNICT983023) and to the Swedish Foundation for Strategic Research for financial support. P. Busson acknowledges the financial support from the Swedish Research Council for Engineering Science (TFR, grant 95-807).

References

[1] H. Motschmann, T. Penner, N. Armstrong, and M. Enzenyilimba. *J. Phys. Chem*, **97**, p. 3933, 1993.
[2] R.B. Meyer, L. Liebert, L. Strzeleki, and P. Keller. *J. Physique*, **36**, p. L69, 1975.
[3] N. Clark and S.T. Lagerwall. *Appl. Phys. Lett.*, **36** p. 899, 1980.
[4] G. Stegeman and R. Stolen. *J. Opt. Soc. Am. B*, **6**(4), p. 652, 1989.
[5] T.L. Penner, H.R. Motschmann, N.J. Armstrong, M.C. Ezenyilimba, and D.J. Williams. *Nature*, **367**, p. 49, 1994.
[6] M. Lindgren, D.S. Hermann, J. Örtegen, P.-O. Arntzen, U.W. Gedde, A. Hult, L. Komitov, S.T. Lagerwall, P. Rudquist, B. Stebler, F. Sahlén, and M. Trollsås. *J. Opt. Soc. Am. B*, **15**(2), p. 914, 1998.
[7] V.S.U. Fazio, S.T. Lagerwall, V. Zauls, S. Schredar, P. Busson, A. Hult, and H. Motschmann. *Eur. Phys. J. E*, 2000. In printing, xxx.lanl.gov/abs/cond-mat/9912145.
[8] M. Trollsås, C. Orrenius, F. Salhén, U.W. Gedde, T. Norin, A. Hult, D. Hermann, P. Rudquist, L. Komitov, S.T. Lagerwall, and J. Lindström. *J. Am. Chem. Soc.*, **118**, p. 8542, 1996.
[9] M. Trollsås, F. Sahlén, U.W. Gedde, A. Hult, D. Hermann, P. Rudquist, L. Komitov, S.T. Lagerwall, and B. Stebler. *Macromol.*, **29**(7), p. 2590, 1996.
[10] D.S. Hermann, P. Rudquist, S.T. Lagerwall, L. Komitov, B. Stebler, M. Lindgren, M. Trollsås, F. Sahlén, A. Hult, U.W. Gedde, C. Orrenius, and T. Norin. *Liq. Crys.*, **24**(2), p. 295, 1998.
[11] P.N. Prasad and D.J. Williams. *Introduction to nonlinear optical effects in molecules and polymers*. John Wiley & Sons, 1991.
[12] David Sparre Hermann. *Interaction of light with liquid crystals*. PhD thesis, Göteborg University and Chalmers University of Technology, 1997.
[13] J. Jerphagnon and S.K. Kurtz. *J. Appl. Phys.*, **41**(4), p. 1667, 1970.
[14] M.J. Weber. *CRC handbook of laser science and technology*, volume III: Optical materials. CRC Press Inc., Florida, 1986.

[15] V.S.U. Fazio, S.T. Lagerwall, P. Busson, A. Hult, and H. Motschmann. *Appl. Phys. Lett.*, **77**(3), p. 319, 2000.
[16] A. Ulman. *An introduction to ultrathin organic films: from Langmuir-Blodgett to self-assembly*. Academic Press Boston, 1991.